SUPPLEMENTARY INTRODUCTION:

DiGeorge Syndrome (DGS) is a relatively common (about 1 in every 4000 live births) primary immunodeficiency defined by chromosomal deletion of 22q11.2 in 90% of DGS patients.[1] The most common contiguous gene deletion syndrome known, DGS results from in-utero midline interruptions that occur during the development of the branchial-pharyngeal complex. As such, common clinical findings include congenital heart disease, hypoparathyroidism (hypocalcemia), velofacialpharyngeal defects and thymic hypoplasia.[2, 3] "Complete" DGS (cDGS) is uncommon. cDGS patients are athymic (less than 2% mature T cells in the periphery) with a high risk for fatality from life-threatening T cell-mediated infections during the early infantile period, similar to that of Severe Combined Immunodeficiency (SCID). The majority of DGS patients, however, are classified as "partial" (pDGS), defined by the presence of mature T cells that range from moderately low for age to normal, and by recurrent mild to moderate infectious processes, usually of the respiratory tract and due to non-opportunistic organisms. During advancing childhood, pDGS patients have the potential for relatively stable T cell levels.[4] Moreover, they appear to have preservation of mitogen-induced T cell proliferative responses and the capacity for antigen-specific cellular and humoral responses.[5] In contrast to cDGS, bone marrow or thymus transplantation is not indicated in pDGS.[6, 7]

Remarkably, midline-organ defects and developmental impairments vary for each organ involved and across patients, resulting in differing degrees of severity. To date, a definitive DGS genotype-phenotype correlation cannot explain the clinical or immunologic differences found in DGS patients. Other organ distortions not derived from branchial-pharyngeal complex impairments and non-T-cell immune defects have also been identified. One subset of pDGS patients exhibits humoral defects and autoimmune disease.[8, 9] Neurocognitive-psychiatric disorders, including autism, attention deficit, anxiety and learning disorders, are found in others, with up to 30% of adolescents and adults exhibiting schizophrenia-like psychosis. The precise etiologies of these neuropsychiatric deficits remain obscure.[10, 11]

SUPPLEMENTAL METHODS:

Proteins, antibodies and chemical reagents

Human recombinant ICAM-1 protein was purchased from Novoprotein (Summit, NJ). Restriction enzymes (*EcoRI*, *BbsI*, *PacI,* and *XhoI)* were purchased from Thermo Fisher Scientific (Waltham, MA). Antibody (Ab) sources are as follows: Anti-LFA-1 (clone mAb24, Hycult Biotech); Anti-LFA-1 (clone KIM127, ATCC); anti-CD3 (clone OKT3, Biolegend); anti-CD45 (clone J.33, Beckman Coulter); anti-CD56 (clone HCD56, Biolegend); anti-CD11a (clone HI111, BD); anti-CD18 (clone 6.7, BD); anti-CD54 (clone HA58, BD); anti-NKG2D (clone 1D11, Biolegend); anti-CD16 (clone 3G8, Biolegend, or clone B73.1, BD); anti-CD107a (clone H4A3, ebioscience); anti-β-tubulin (clone TUB 2.1, Sigma-Aldrich); anti-p-Vav1 (Polyclone, Y174, Abcam); anti-perforin (clone δG9, Biolegend, or clone B-D48, Biolegend); Biotinylated anti-CD244 (clone eBioC1.7, ebioscience); anti-CrkL (clone 32H4, Cell Signaling Technology, or polyclone, Santa Cruz Biotechnology); anti-Tbx1 (polyclone, Abcam); anti-Erk2 (clone E460, Abcam); and mouse IgG1 isotype (clone MOPC 21, Sigma-Aldrich). Phorbol 12-myristate 13-acetate (PMA) and ionomycin were from Sigma Aldrich. The 1,2-Dioleoyl-sn-Glycero-3-Phosphocholine (DOPC), 18:1 Biotinyl Cap PE 1,2-dioleoyl-sn-glycero-3-phosphoethanolamine-N-(cap biotinyl), and 1,2-Dioleoyl-sn-Glycero-3-[(N-(5-amino-1-carboxypentyl) iminodiacetic acid) succinyl] (Nickel salt) (DOGS-NTA) were from Avanti Polar Lipids, Inc. Carboxyfluorescein succinimidyl ester (CFSE) and eFluor 670 dyes were purchased from Life Technologies and ebioscience, respectively. Anti-NKG2D, anti-CD16, ICAM-1 and mouse IgG1 isotype were biotinylated using EZ-Link NHS-PEG4-Biotin and Biotinylation Kits (Pierce). Biotinylated proteins were labeled with Alexa Fluor dyes (Life Technologies) and further purified by high-performance liquid chromatography (HPLC).

Cells

Human CD16-KHYG-1 NK cell line (a gift of D.A. Evans, Harvard Medical School) was cultured in RPMI 1640 medium (Invitrogen) supplemented with 10% heat-inactivated fetal bovine serum (FBS, Atlanta Biologicals), 1 mM Sodium Pyruvate

(Mediatech), 25 mM HEPES (Invitrogen), 2 mM L-Glutamine (Invitrogen), 100 U/ml Penicillin, 100 mg/ml Streptomycin, 0.1 mg/ml Primocin (Invivogen), 100 U/ml IL-2 and 1 μg/ml cyclosporine A (CsA) (Sigma-Aldrich).[12] CD16-KHYG-1 cells were transduced with lentiviral vector encoding CrkL shRNA or Scramble shRNA. To induce shRNA expression, transduced CD16-KHYG-1 cells were treated with 2 μg/ml Doxcycline (Dox). Human K562 and Raji cell lines were cultured in RPMI 1640 supplemented with 10% heat-inactivated FBS, 1 mM Sodium Pyruvate, 1X non-essential amino acids (Invitrogen), 25 mM HEPES, 2 mM L-Glutamine, 100 U/ml Penicillin, and 100 mg/ml Streptomycin. S2 and S2-ICAM-1 cells (a gift from E. O. Long, National Institutes of Health) were cultured in Schneider's Medium (Invitrogen) supplemented with 10% heat-inactivated FBS, 100 U/ml Penicillin and 100 mg/ml Streptomycin. Blood samples from pDGS patients and healthy control subjects were drawn for research purposes at the Texas Children's Hospital under a Baylor College of Medicine IRB protocol with informed consent. PBMCs were isolated from whole blood by density centrifugation using Ficoll-Paque. NK cells were isolated by negative selection using an NK isolation kit (Miltenyi Biotec). Chromosome 22q11.2 deletion in each DiGeorge syndrome patient was validated by fluorescent in situ hybridization (FISH) and/or chromosomal microarray analysis (CMA). PBMC expression of CrkL, Tbx1 and Erk2 protein was further analyzed by intracellular staining.

Plasmids

The plasmids sources were as follows: pLenti-mGFP, pLenti-CrkL-mGFP and packaging vectors (Origene, MA); shRNA constitutive expression vector pUGM, psiCheck2 vector, shRNA inducible expression vector and its package plasmids, including pCMV-VSVg, RSV-rev, pMDL-gag/pol and pAdvantage (S. Kissler, Harvard Medical School); and CrkL-EYFP vector (B.J. Mayer, UConn Health Center).

Luciferase reporter assay

ShRNAs were designed by the hairpin generation program 'RNAi oligo retriever' (http://cancan.cshl.edu/RNAi_central/RNAi.cgi?type=shRNA)[13] and synthesized in IDT (San Jose, CA). The following shRNA sequences were used: CrkL shRNA oligo #1: 5'-tgctgttgacagtgagcgcagtcacaaggatgaatataaatagtgaagccacagatgtatttatattcatccttgtgactttgcctactgcctcgga-3'; CrkL shRNA oligo #2: 5'-tgctgttgacagtgagcgcttcctgtcccttatgtcgaaatagtgaagccacagatgtatttcgacataagggacaggaattgcctactgcctcgga-3'; CrkL shRNA oligo #3: 5'-tgctgttgacagtgagcgctcccagaacctgctcatgcattagtgaagccacagatgtaatgcatgagcaggttctgggattgcctactgcctcgga-3'; CrkL shRNA oligo #4: 5'-tgctgttgacagtgagcgccctgtctttgcgaaagcaatctagtgaagccacagatgtagattgctttcgcaaagacaggttgcctactgcctcgga-3'; Scramble shRNA oligo: 5'-tgctgttgacagtgagcgaattctccgaacgtgtcacgtttagtgaagccacagatgtaaacgtgacacgttcggagaatctgcctactgcctcgga-3'. PsiCheck2 and luciferase reporter assays used for shRNA cloning were described previously.[14] Each shRNA oligo was amplified with primers as follows: 5'-cagaaggctcgagaaggtatattgctgttgacagtgagcg-3' (forward primer with an *XhoI* site) and 5'-ctaaagtagccccttgaattccgaggcagtaggca-3' (reverse primer with an *EcoRI* site). The lentiviral constitutive expression pUGM vector encoding Green Fluorescent Protein (GFP) was digested with *EcoRI* and *XhoI*. The backbone was recovered and annealed with individual *EcoRI* and *XhoI* digested shRNA oligo. Wild-type CrkL sequence was amplified from the CrkL-EYFP vector.[15] Luciferase reporter assays were performed using Promega's dual luciferase reporter assay system. After adding luciferin substrate, firefly and renilla luminescence was measured in an Infinite M200 (Tecan). ShRNA silencing efficiency was measured by the percentage of renilla luminescence signal according to the equation:

Relative luminescence (%) $= \frac{\frac{a}{b}}{\frac{c}{d}} \times 100$, in which a is the intensity of renilla from pUGM and psiCheck2 co-transfected 293T cells; b is the intensity of renilla from psiCheck2 alone transfected 293T cells; c is the intensity of firefly from pUGM and psiCheck2 co-transfected 293T cells; and d is the intensity of firefly from psiCheck2 alone transfected 293T cells. The ratio of renilla and firefly luminescence in 293T cells transfected with *CrkL* luciferase reporter only was set to 100%.

Inducible CrkL knockdown construct

The strategy for generating inducible knockdown shRNA has been described.[14, 16] Briefly, effective shRNA oligo (CrkL shRNA oligo #1) was identified by Luciferase reporter assay. To generate the inducible knockdown construct, CrkL and scramble oligos containing *BbsI* and *XhoI* overhangs were synthesized by IDT (San Jose, CA). Oligo sequences were as follows: CrkL sense: 5'-tccccagtcacaaggatgaatataaa ttcaagagatttatattcatccttgtgactgtttttctcgag-3'; CrkL anti-sense: 5'-tcgagaaaaacagtcacaaggatgaatataaatctcttgaatttatattcatccttgtgactg-3'; Scramble sense: 5'-tcccaattctccgaacgtgtcacgttttcaagagaaacgtgacacgttcggagaatttttttctcgag-3'; Scramble anti-sense: 5'-tcgagaaaaaaattctccgaacgtgtcacgtttctcttgaaaacgtgacacgttcggagaatt-3'. Because the FH1t-UTG vector lacks human H1-promoter with a tet-operator (H-tetO promoter), sense and anti-sense strands were annealed and inserted into *BbsI* and *XhoI* digested pH1tet-flex vector. The sequence fragment that included human H-tetO promoter with the effective shRNA was recovered by *Pac*I digestion and cloned into the inducible FH1t-UTG vector. Positive clones were confirmed by sequencing.

Lentivirus generation and cell transduction

CrkL shRNA- and scramble shRNA-containing lentiviral vectors were generated by co-transfecting 293T cells with four package plasmids (pCMV-VSVg, RSV-rev, pMDL-gag/pol, and pAdvantage). Viral particles were harvested at 57,400 g at 4°C for 90 min. Concentrated virus was titrated by infecting 4 x 10^5 293T cells. On day 2, transduced 293T (GFP^+) cells were analyzed by flow cytometry to determine viral titer according to the following equation.

Virus titer = Percentage of GFP^+ cells (%) × cell number × virus dilution

CD16-KHYG-1 cells were spin-infected (1,000 g for 2 hours) with lentivirus in the presence of 8 μg/ml polybrene (Sigma-Aldrich) at a multiplicity of infection (MOI) of 20. GFP positive CD16-KHYG-1 cells were sorted by FACSAriaII (BD). To overexpress CrkL in pDGS patient samples, PBMCs or purified NK cells were spin-infected with pLenti-mGFP or pLenti-CrkL-mGFP lentivirus in the presence of 10 μg/ml polybrene for 2 hours at a MOI of 20-42. Transduced cells were cultured with 10 ng/ml IL-15 and 100 U/ml IL-2 for 2 days and were used within 48 hours.

Western blotting

Wild type, CrkL-shRNA KD, and Scramble shRNA CD16-KHYG-1 cells were untreated or treated with 2 μg/ml Doxycycline (Dox) for 3-4 days. 5 x 10^6 cells were lysed in RIPA buffer supplemented with 10% protease inhibitor cocktail (Sigma-Aldrich) on ice for 30 min. Target proteins were probed with antibodies against CrkL (1:1000, Cell Signaling Technology) and Tubulin (1:2000, Sigma-Aldrich), and visualized under an Odyssey CLx (LI-COR). To quantify CrkL expression levels, Image J (NIH) was used to measure CrkL and tubulin intensities with background subtraction. Calculation of the percentage of knockdown was made according to the following equation:

Relative CrkL protein level (%) $= \frac{\frac{a}{b}}{\frac{c}{d}} \times 100$, in which a is the intensity of CrkL from CD16-KHYG-1 cells transduced with shRNA-KD; b is the intensity of CrkL from wild type CD16-KHYG-1 cells; c is the intensity of tubulin from CD16-KHYG-1 cells transduced with shRNA-KD; and d is the intensity of tubulin from wild-type CD16-KHYG-1 cells.

Healthy control or pDGS PBMCs were lysed in RIPA buffer containing 10% protease inhibitor cocktail on ice for 30 min. Lysates were probed with antibodies against CrkL (1:2000, Santa Cruz), Tbx1 (1:200, Abcam), ERK2 (1:1000, Abcam), and Tubulin (1:2000, Sigma-Aldrich).

NK-Target Conjugation assay

NK-Target conjugation assays were described previously.[17] Briefly, NK cells and K562 cells were labeled at room temperature for 5 min with 5 μM CFSE and 2.5 μM eFluor 670, respectively. Cells were then washed three times with PBS. Similarly, S2-ICAM-1 cells were washed once with HBSS, stained with 2.5μM eFluor 670 and then coated with anti-S2 serum (1:10,000) at room temperature. 10^5 NK and 10^5 target cells were mixed at 37°C for the indicated duration times. Cells

were fixed by freshly prepared 0.5% paraformaldehyde for 15 min at room temperature. After a gentle vortex, cells were analyzed in a LSR Fortessa flow cytometer. Conjugates were defined as two-color positive cells.

CD107a degranulation assay

CD107a degranulation assay was described previously.[18] Briefly, 10^5 NK cells or PBMCs were unstimulated, or stimulated with either 2 x 10^5 target cells or 100 ng/ml PMA plus 1µg/ml ionomycin. Cells were mixed at 300 rpm for 3 min. Cells were then incubated at 37°C in 5% CO_2 for 2 hours in the presence of PE-Cy5 conjugated anti-CD107a. For PBMCs, 1 µl/ml Golgistop was added, and cells were further stained with anti-CD3, CD56 mAbs to identify NK cells. Cells were washed twice with PBS supplemented with 2% FBS and 5 mM EDTA, re-suspended in the washing buffer and analyzed in the LSR Fortessa flow cytometer.

Chromium^{51} release assay

NK cell cytotoxicity toward K562 or Rituximab-coated Raji cells was determined using previously described 4-hour ^{51}Cr-release assays.[19] Briefly, K562 and Raji target cells were labeled with ^{51}Cr at 37°C for 1 hour. For ADCC assays, Raji cells were incubated with 20 µg/ml Rituximab on ice for 30 min. K562 and Rituximab coated Raji cells were re-suspended at 1 x 10^5/ml in RPMI medium with 10% FBS. 1 x 10^4 K562 or Rituximab-coated Raji cells were incubated with serial diluted NK cells at 37^{o}C for 4 hours. For NK cell cytotoxicity using PBMCs, 0.5 x 10^4 target cells were used. Radioactivity was measured on a Topcount NXT (Perkin Elmer, MA).

Quantification of LFA-1 conformation and cytolytic machinery by flow cytometry

All flow cytometry measurements were performed on a LSR Fortessa flow cytometer (BD Biosciences). Quantification of activated/intermediate LFA-1 by mAb24/KIM127 was described previously.[20] Briefly, 2 x 10^5 PBMCs from healthy control

or pDGS patients were mixed with 2 x 10^5 K562 cells at 37°C for indicated times. For cell surface staining of LFA-1, cells were stained with mAb24 or KIM127. After two washes with PBS 2% FBS, cells were stained with Alexa Fluor 488 conjugated anti mouse IgG1 antibody. Cells were then washed, and further stained with viability dye (Life Technologies), anti-CD45, anti-CD3, anti-CD56, and anti-CD11a to define live NK cells, percentage of live NK cells with activated/intermediate LFA-1, and total LFA-1 expression. For intracellular molecule staining, PBMCs transduced with either control GFP or CrkL-GFP were stimulated with K562 in the presence of Golgistop and Brefeldin A for 6 hours. Cells were fixed with cytofix/cytoperm buffer (BD) at room temperature for 15 min and washed with perm/wash buffer (BD). Cells were then intracellularly stained with anti-IFN-γ, TNF-α, perforin (clone B-D48), and granzyme B mAbs in PBS 2% FBS, and analyzed in a LSR Fortessa flow cytometer.

Image Acquisition and Analysis

NK-target conjugates were prepared on the poly-lysine coated slides, as described previously.[21] Three-dimensional (3D) confocal images were acquired to visualize perforin, CrkL, phos-Vav1, β-tubulin, and F-actin.[21] z-series around lipid bilayers were used to quantify polarization of lytic granules on bilayers. Bilayer focal planes were defined by maximal signal intensity by 3D image reconstruction. All images were acquired with a Leica time-gated STED microscope. Data was analyzed with Volocity (PerkinElmer), Imaris (Bitplane) or LAS AF software (Leica).

siRNA transfection

SiRNA against CrkL (5'-gucacaaggaugaauauaa-3') and Scramble siRNA (5'-uucuccgaacgugucacgu-3') were obtained from Thermo Fisher Scientific. 100 U/ml IL-2 activated primary NK cells were transfected with 300 pmol CrkL siRNA or scramble siRNA on an Amaxa nucleofector (Lonza, Basel) using the U-001 program as described.[21] On day 2, cells were mixed with K562 target cells and lytic granule polarization was visualized by confocal microscopy.

Glass-supported planar lipid bilayers

Planar lipid bilayers were prepared by fusing small liposome droplets with clean glass coverslips as described.[22] Briefly, liposome were trapped in a μ-Slide VI $^{0.4}$ chamber (Ibidi, Germany). Lipid bilayers were first blocked with 5% Casein for 30 min and then incubated with 6.3 nM Streptavidin (Life Technologies) for 20 min. After extensive washing with imaging buffer (HEPES-buffered saline), bilayers were incubated with biotinylated antibodies conjugated with Alexa Fluor dyes at room temperature for 30 min. After a second wash with imaging buffer, bilayers were blocked with 2.5 μM D-biotin to saturate streptavidin binding sites. Cells were activated on the bilayers for 10-15 min (CD16-KHYG-1 cells) or 60 min (primary NK cells). For bilayers using CD16-KHYG-1 cells, bilayer densities were: 150 ng/ml anti-CD16-Alexa Fluor 568, 150 ng/ml anti-NKG2D-Alexa Fluor 568, 150 ng/ml anti-2B4, 500 ng/ml ICAM-1, and 500 ng/ml ICAM-1-Alexa Fluor 647. For bilayers using primary NK cells, bilayer densities were: 75 ng/ml anti-CD16-Alexa Fluor 568, 150 ng/ml anti-NKG2D-Alexa Fluor 568, 250 ng/ml ICAM-1-Alexa Fluor 647, 150 ng/ml anti-2B4, 18 nM anti-CD107a Fab-Alexa Fluor 647.

Stimulated Emission Depletion (STED) imaging of planar lipid bilayers

CD16-KHYG-1 cells were stimulated on lipid bilayers containing proteins as indicated. Cells were then fixed and permeabilized, followed by Alexa Fluor 488 antibody staining against perforin and Alexa Fluor 532 phalloidin staining against F-actin. A Leica TCS SP8 microscope with a time-gated stimulated emission depletion (STED) module with a 592 nm depletion laser was used to achieve super-resolution visualization of F-actin and perforin.[23]

Statistical analysis

Unpaired or paired two-tailed t-tests were performed using Prism software (GraphPad Software, Inc.).

SUPPLEMENTARY DISCUSSION:

All of our cohorts of 18 patients (Supplementary Tables 1 and 2) were classified as pDGS (none cDGS). Restoration of NK cell function was assayed in 8 (Supplementary Table 1). NK cell function was assayed in 11 patients (Supplementary Table 2). One patient (P1) was studied in both experimental arms. All patients in the cohort had recurrent respiratory infections and cognitive learning delays, in addition to a range of velopharyngeal abnormalities and facies consistent with pDGS. None had hypoparathyroidism. One patient (P9) had non-verbal autism. Two patients had autoimmune thyroiditis, one had viral cutaneous syndrome (warts and molluscum), one had cutaneous fungal infection with seborrheic dermatitis, and four had confirmed metapneumoviral sinopulmonary disease. One patient (P14) had co-existing IgA deficiency, defined as IgA less than 10 mg/dL at 9 years of age but was without autoimmune disease. Immunologic findings ranged from lymphopenia with abnormally low CD3 T cells to normal absolute lymphocyte count and normal T cell percentages and absolute numbers for age.

All of the patients studied for functional restoration of NK cells experienced restored function. Results did not appear to relate to peripheral T cell numbers, as four out of the eight patients had abnormally low T cell counts for age while the other four had normal counts. Only one patient (P18) had low NK cell counts. Although P18's absolute number of NK cells was lower than normal (127 vs. 152-595), percentage of NK cells fell within the normal range (10% vs. 7-28%). All patients had B cells counts within the normal range for age. In the 11 patients used for functional analyses, distributions of lymphocyte subsets were at or near normal ranges. Absolute lymphocyte counts, however were relatively low. In all pDGS patients analyzed for LFA-1 activation by mAB24^{+} (6 patients) and KIM 127^{+} (4 patients), antibody staining (percentage and MFI) was lower than in healthy control subjects; two of these patients had cutaneous viral infections (warts, molluscum, and fungal dermatophytosis).

SUPPLEMENTAL FIGURE LEGEND

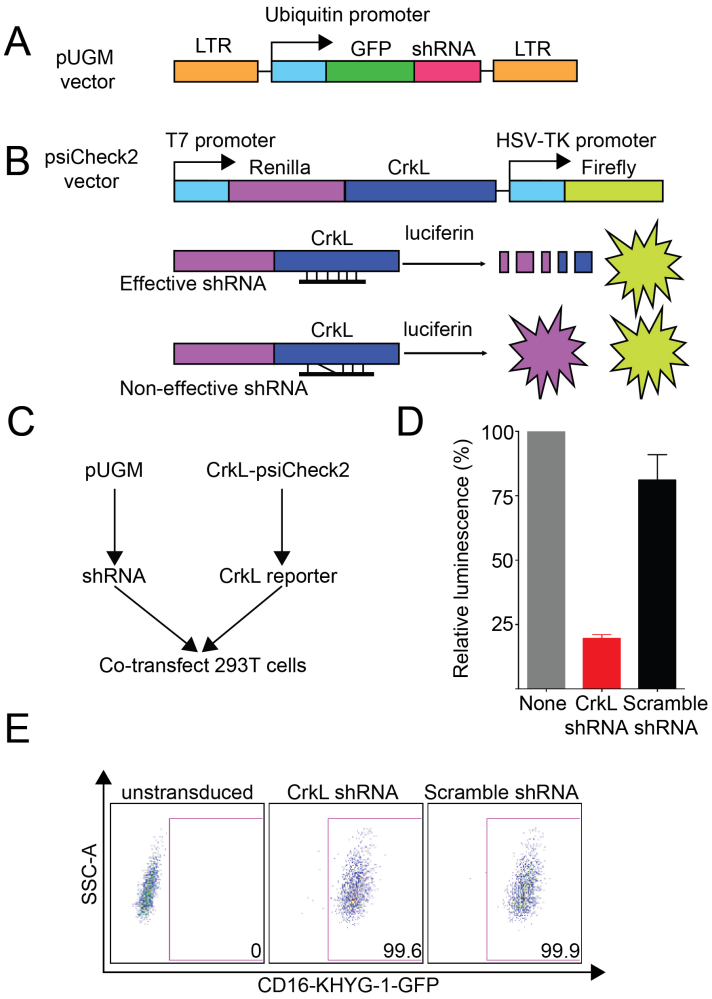

FIG E1. shRNA screening by luciferase reporter assay. A, Schematic diagram of constitutive expression lentiviral vector pUGM, in which ubiquitin promoter drives the expression of GFP (green) and shRNA (red). **B**, Schematic diagram of

psiCheck-2 vector. The Renilla-CrkL fusion mRNA and Firefly mRNA are expressed by T7 and HSV-TK promoters, respectively. **C**, Luciferase reporter assay. 293T cells were co-transfected with *CrkL* luciferase reporter and pUGM vector containing either CrkL shRNA or scrambled shRNA (control). **D**, The percentage of relative luminescence was calculated by the ratio of CrkL shRNA and scrambled shRNA. Data represents two different experiments. **E**, The percentage of GFP positive CD16-KHYG-1 cells transduced with an effective CrkL shRNA inducible lentivirus or scrambled shRNA lentivirus. The GFP positive population was sorted by FACSAriaII (BD).

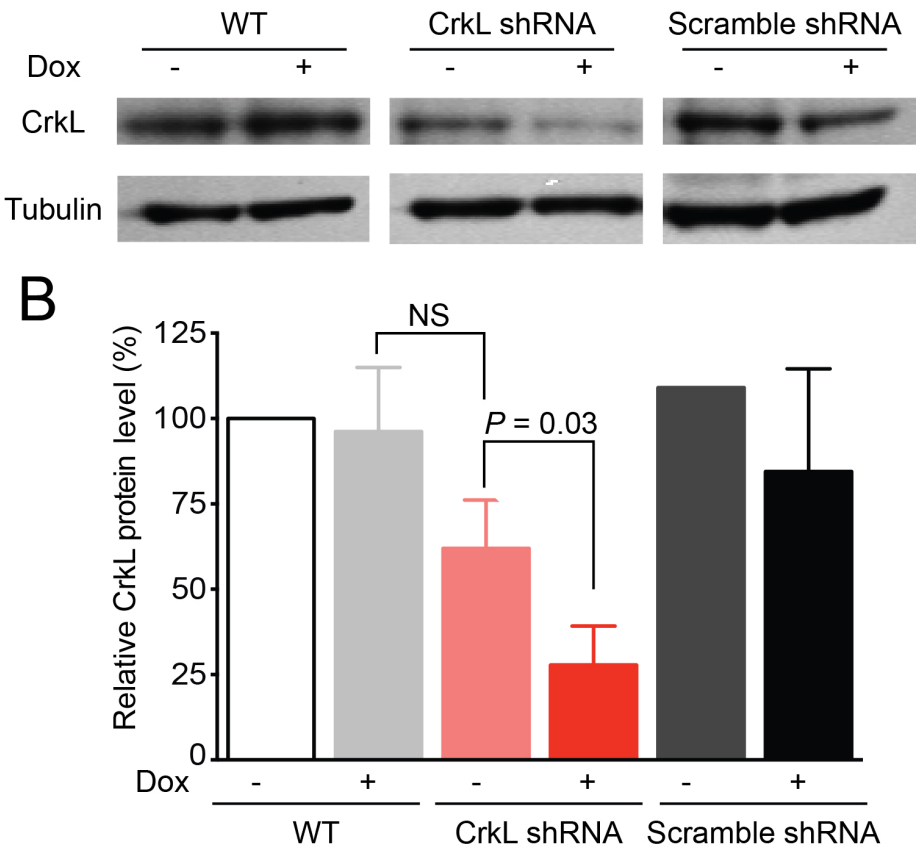

FIG E2. Validation of CrkL inducible knockdown by Western blotting. wild-type (WT), CrkL shRNA(KD), and scrambled shRNA (control) CD16-KHYG-1 cells were treated with doxycycline (Dox, +) or vehicle control (-) for 4 days. **A**, CrkL and loading control (Tubulin) proteins were probed with the antibodies against CrkL and Tubulin, respectively. **B,** Quantification of CrkL protein in WT, CrkL KD, and control CD16-KHYG-1 cells. Error bars show ± standard deviation (s.d.). Data is representative of 3 independent experiments. NS = not significant. *P* value as per Student's *t*-test.

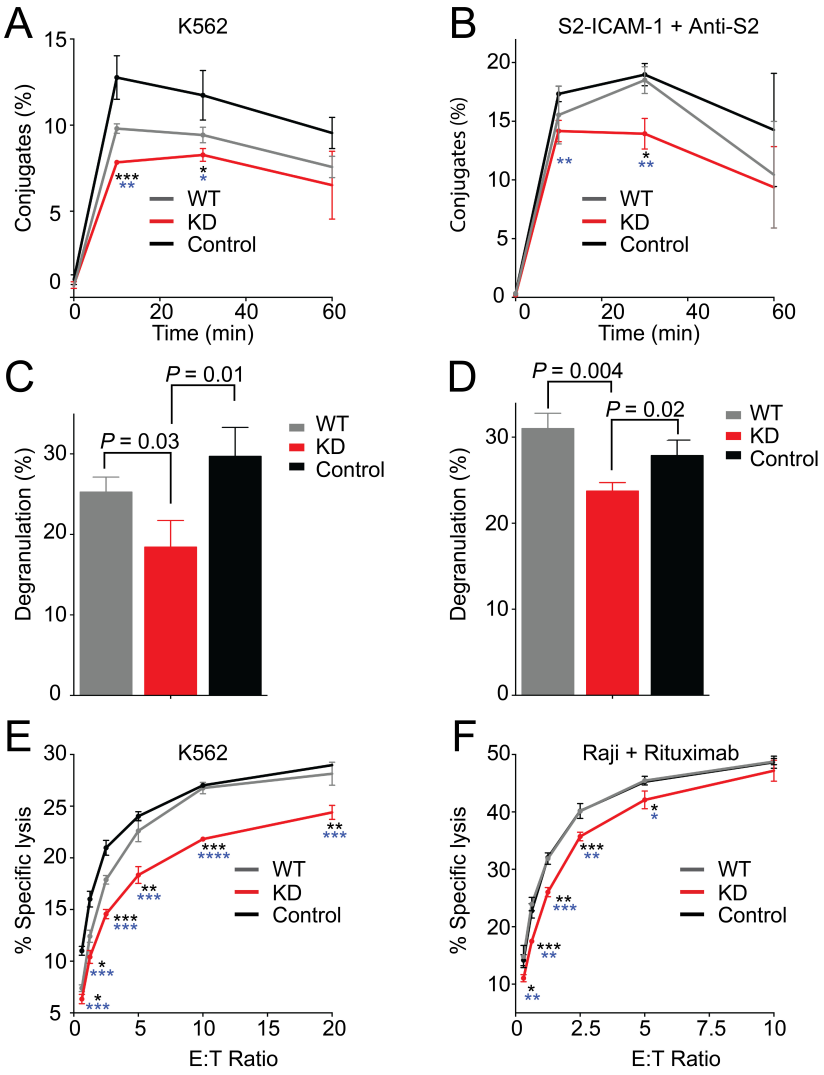

FIG E3. CrkL silencing inhibits NK cell conjugation, degranulation, and cytotoxicity. A and **B**, Percentage of conjugate formation between wild-type (WT), CrkL shRNA (KD), and scrambled shRNA (control) CD16-KHYG-1 cells with susceptible K562 cells (Fig E3, *A*) and anti-S2 serum pre-coated S2-ICAM-1 cells (Fig E3, *B*) at different time points, as

indicated. **C** and **D**, Percentage of CD107a on the surface of NK cells in WT, CrkL KD, and control CD16-KHYG-1 cells were measured after 2-hour incubation with K562 (Fig E3, *C*) or anti-S2 serum pre-coated S2-ICAM-1 cells (Fig E3, *D*). **E** and **F**, Cytotoxicity capability of WT, KD and control lentivirus transduced CD16-KHYG-1 cells was measured by a 4-hour standard ^{51}Cr-release assay. Natural cytotoxicity to susceptible target cells-K562 (Fig E3, *E*) and ADCC assays against rituximab (anti-CD20) pre-coated Raji cells (Fig E3, *F*) were shown at the indicated ratios of effector to target cells (E:T ratio). Data are representative of 4-6 independent experiments. Black stars represent the comparison between KD and WT, and blue stars represent the comparison between KD and control. *$P \leq 0.05$, **$P \leq 0.01$, ***$P \leq 0.001$, ****$P \leq 0.0001$, unpaired Student's *t*-test. Error bars show ± s.d.

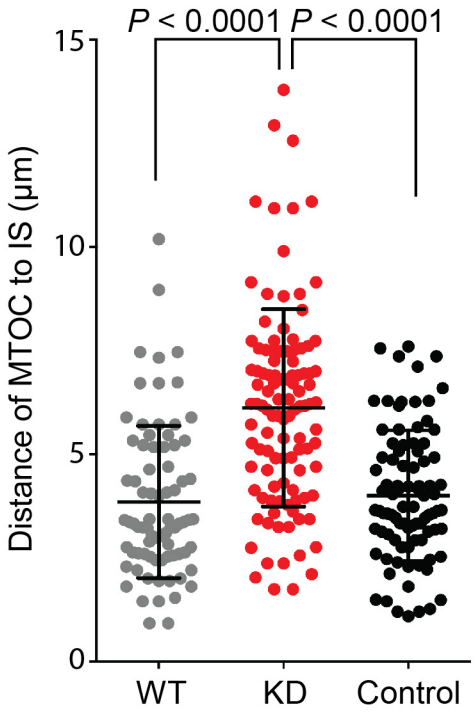

FIG E4. CrkL silencing disrupts lytic granule polarization to the IS formed between NK and anti-S2 serum coated S2-ICAM-1 cells. WT, KD, and control CD16-KHYG-1 cells were conjugated with anti-S2 serum coated S2-ICAM-1 cells. Cells were stained with Abs to visualize perforin (a marker for lytic granules) and β-tubulin (to define the position of MTOC) to quantitatively measure the distance between the MTOC and the IS. Error bars show ± s.d. Data from 3 independent experiments.

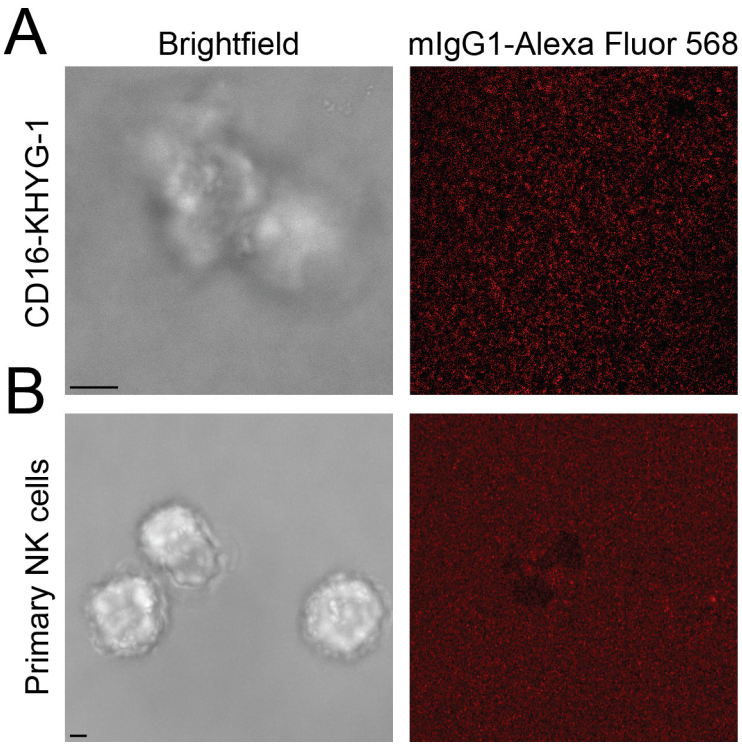

FIG E5. NK cell activating receptors do not form microclusters on bilayers carrying mouse IgG1 isotype control. A and **B**, CD16-KHYG-1 cells (Fig E5, *A*) or human primary NK cells (Fig E5, *B*) were incubated on bilayers carrying the corresponding concentration of mouse IgG1 antibody directly conjugated with Alexa Fluor 568. Both bright field and mouse IgG1-Alex Fluor 568 (red) confocal images are shown. Scale bars represent 3 μm.

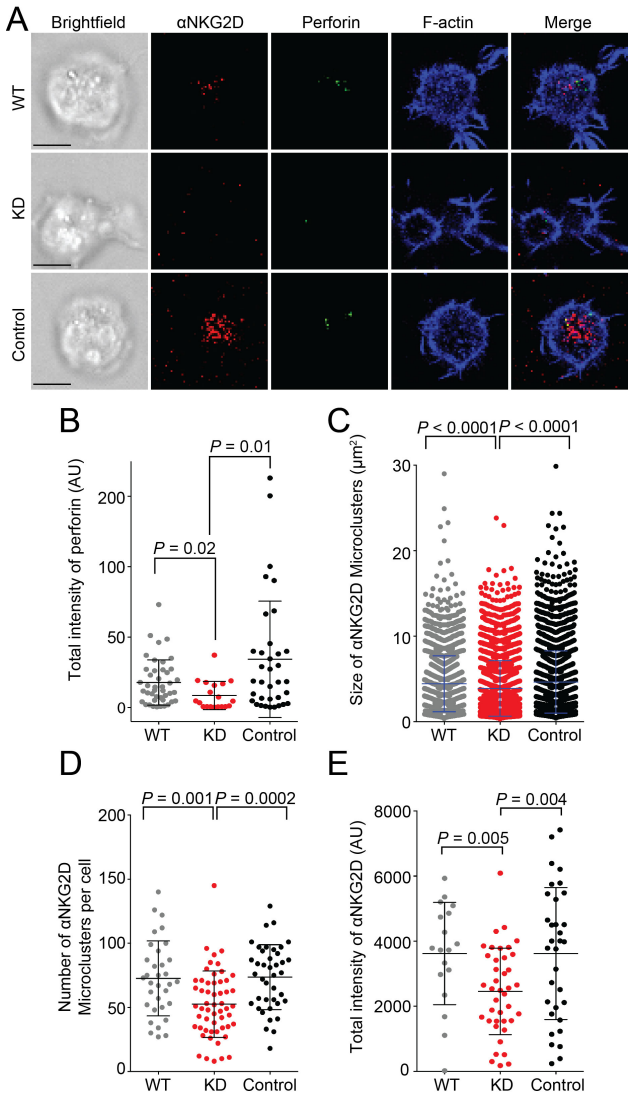

FIG E6. CrkL silencing inhibits anti-NKG2D accumulation and lytic granules polarization under super-resolution STED microscopy. A, Confocal images of WT, KD, and control CD16-KHYG-1 cells on bilayers carrying anti-NKG2D-

Alexa Fluor 568 (red) and unlabeled anti-2B4 in the presence of unlabeled ICAM-1. Fixed and permeabilized NK cells were stained for perforin followed by Alexa Fluor 488-conjugated secondary Ab (green) to visualize lytic granules, and phalloidin-Alexa Fluor 532 (blue) to detect F-actin. Super-resolution STED images of F-actin and perforin were obtained at *x*-*y* plane by a Leica time-gated STED microscope using a 592 depletion laser. The lipid bilayer focal plane was defined by the highest intensity anti-NKG2D-Alexa Fluor 568 signals. Scale bars represent 1.5 μm. **B**, Quantification of the total intensity of polarized perforin. **C** to **E**, Quantification of the size (Fig E6, *C*), number (Fig E6, *D*) and total intensity (Fig E6, *E*) of anti-NKG2D microclusters on bilayers. Error bars indicate ± s.d. Data represent 6 independent experiments.

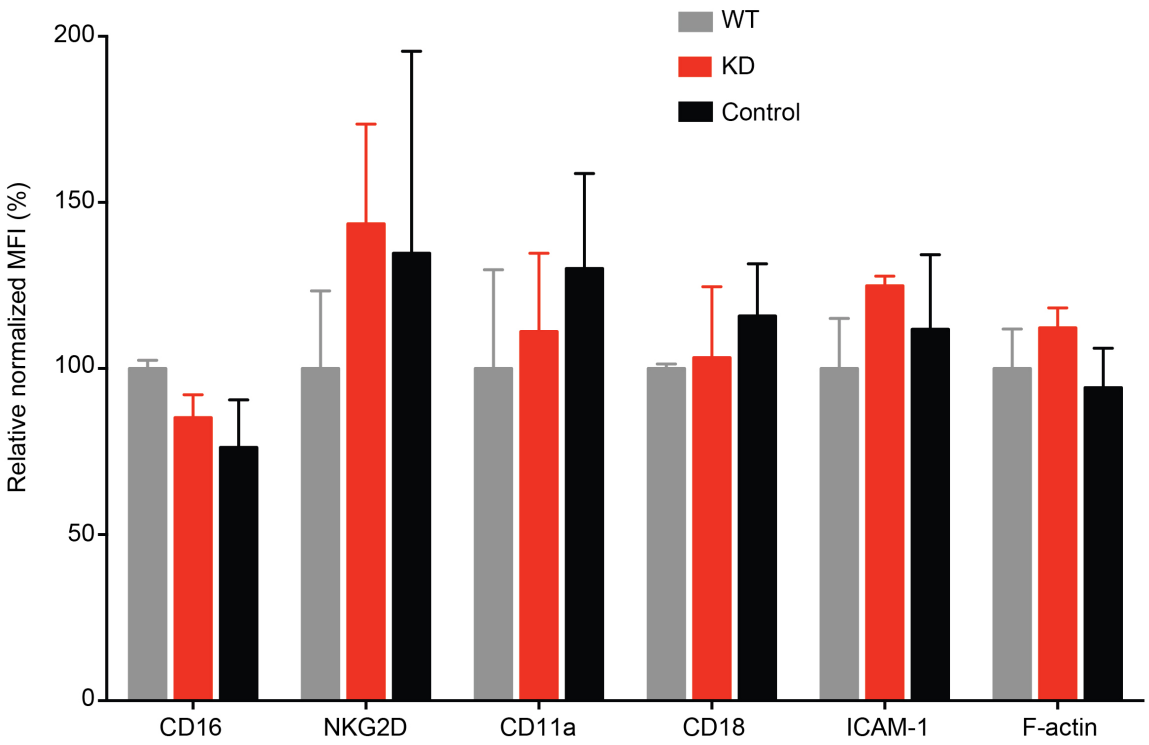

FIG E7. Comparable expression levels of activating receptors, adhesion molecules, and F-actin in CrkL-silenced NK cells. Quantification of activating receptors CD16 and NKG2D, adhesion molecules CD11a, CD18, and ICAM-1, and F-actin expression on WT, KD, and control CD16-KHYG-1 cells by flow cytometry. CD16, NKG2D, CD11a, CD18, and ICAM-1 expression were quantified by mAb staining of CD16-KHYG-1 cells as described in Methods. F-actin expression was quantified using Alexa Fluor 568 phalloidin. Error bars indicate ± s.d. Data represent 2 independent experiments.

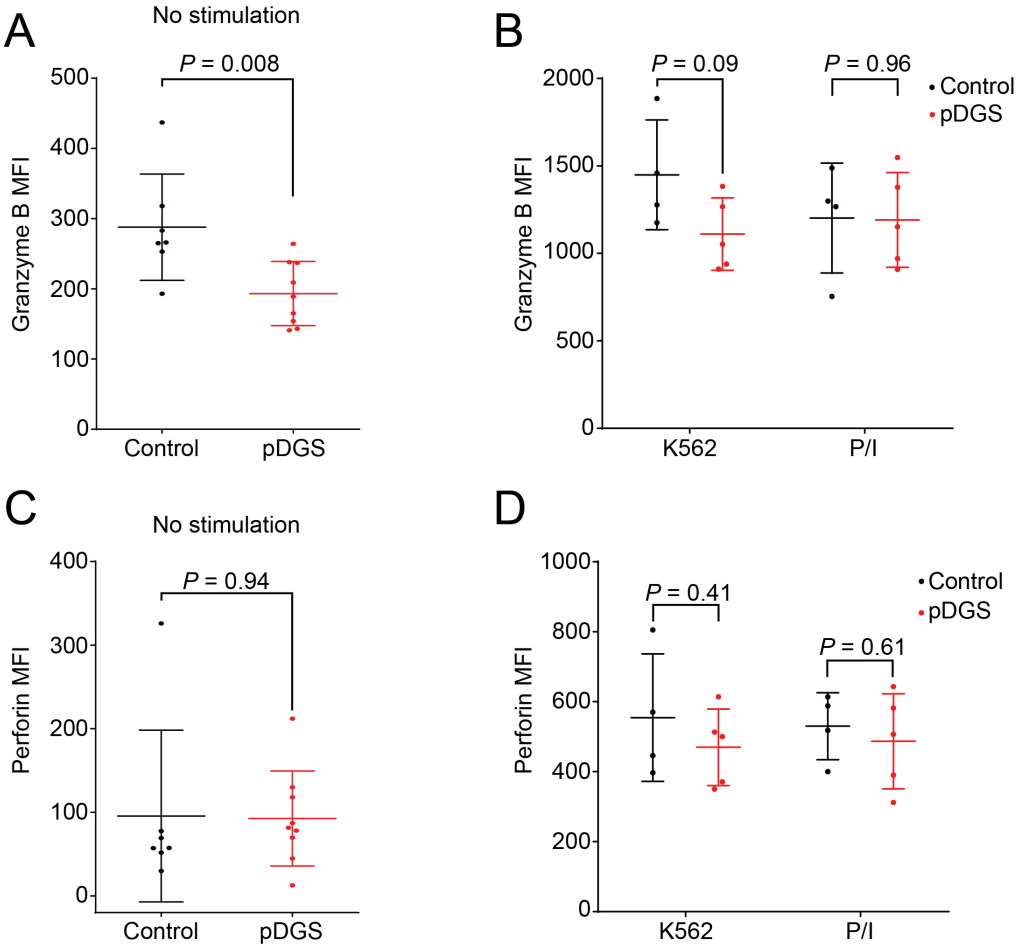

FIG E8. Lytic machinery content in NK cells from pDGS patients. A and **B**, MFI (as measured by flow cytometry) of granzyme B in resting (A) and stimulated (B) NK cells from controls and pDGS patients. **C** and **D**, MFI of perforin in resting (C) and stimulated (D) NK cells. PBMCs were stimulated by K562 or PMA plus ionomycin (P/I) for 2 hours, as indicated. Error bars indicate ± s.d.

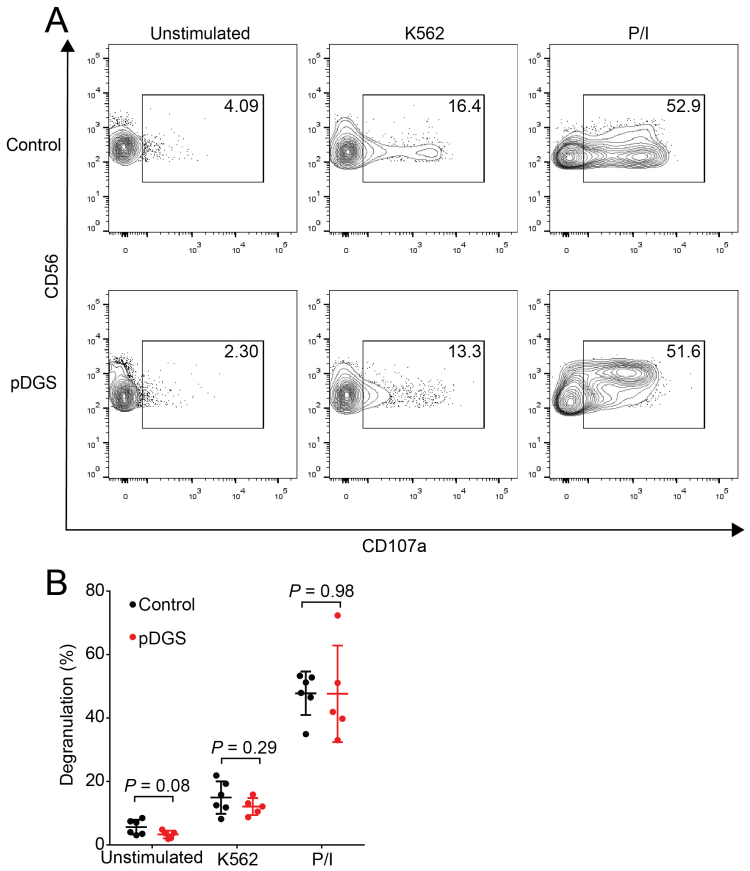

FIG E9. CD107a degranulation on NK cells from pDGS patients. **A**, FACS plot depicting CD107a degranulation of healthy control and pDGS NK cells in response to K562 targets and PMA plus ionomycin (P/I). **B**, Quantitative result of CD107a degranulation on NK cells from 6 controls and 5 pDGS patients.

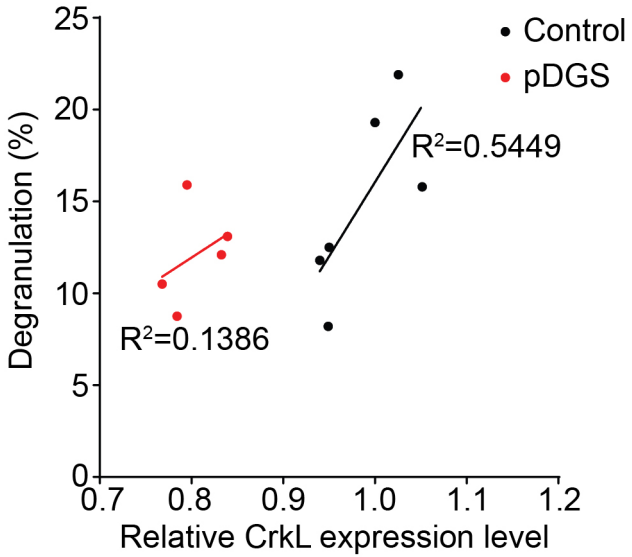

FIG E10. Surface CD107a staining correlates positively with CrkL expression in both healthy control and pDGS NK cells. CrkL expression was measured by flow cytometry. Correlation was analyzed with linear regression using Graphpad software.

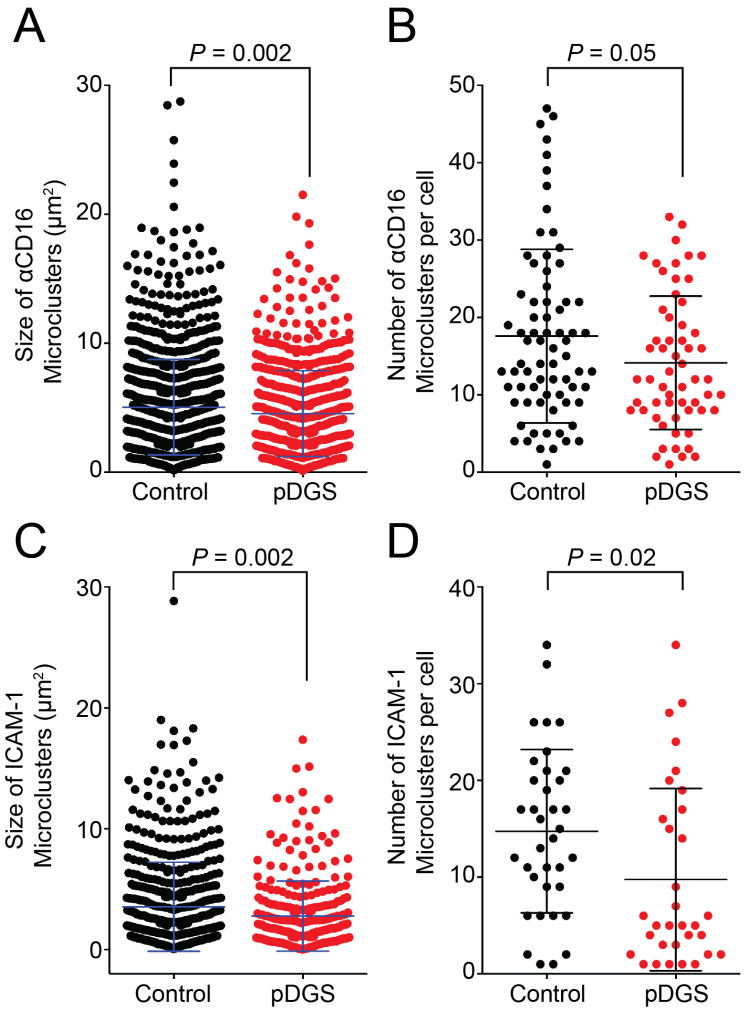

FIG E11. Decreased anti-CD16 and ICAM-1 microcluster accumulation in primary NK cells from pDGS patients. Primary NK cells from pDGS patients and healthy control subjects were stimulated on bilayers carrying ICAM-1-Alexa Fluor 647 and anti-CD16-Alexa Fluor 568. **A** and **B**, Quantification of size (Fig E11, *A*) and number (Fig E11, *B*) of anti-CD16

microclusters. **C** and **D**, Quantification of size (Fig E11, *C*) and number (Fig E11, *D*) of ICAM-1 microclusters. Error bars indicate ± s.d. Data represent 2-4 independent experiments.

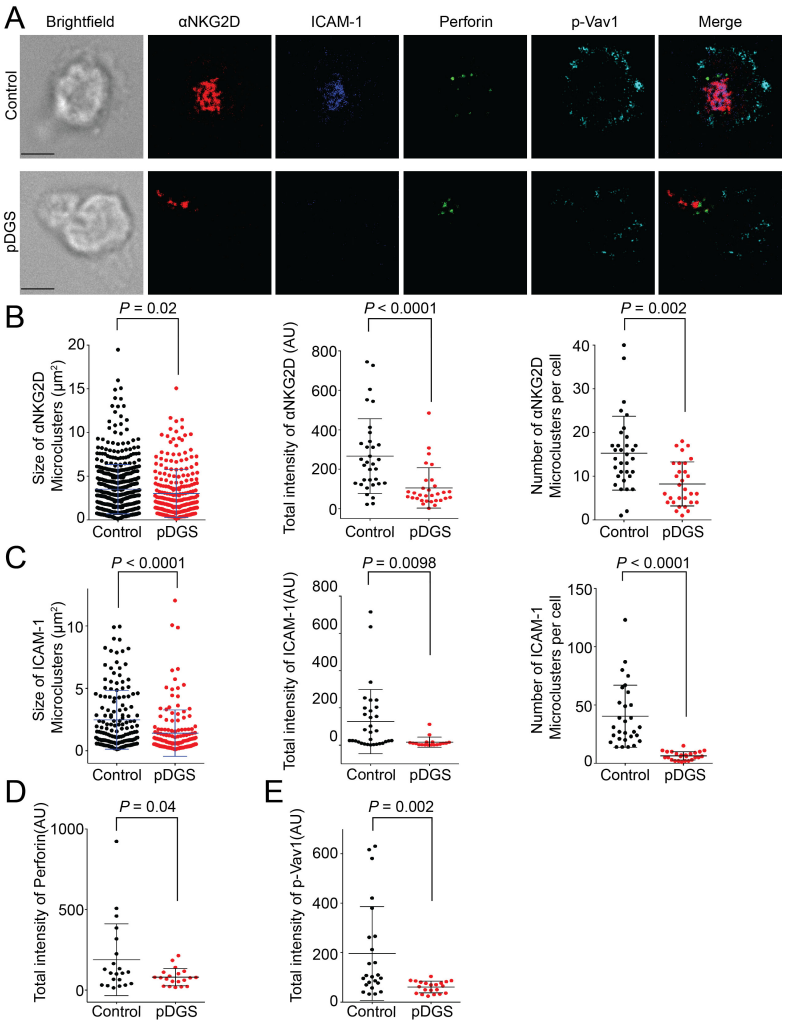

FIG E12. Defects in lytic granule polarization, NKG2D and LFA-1 clustering, and pVav-1 accumulation at the pDGS NK cell cytotoxic IS. A, Confocal images of primary NK cells from healthy control subjects (Control) and pDGS patients (pDGS) stimulated on bilayers carrying anti-NKG2D-Alexa Fluor 568 (red) and unlabeled anti-2B4 in the presence of ICAM-

1-Alexa Fluor 647 (blue). Cells were stained with anti-perforin-Alexa Fluor 488 (green) and anti-pVav-1-Alexa Fluor 405 (cyan). **B** and **C**, Quantification of the size, total intensity and number of anti-NKG2D (Fig E12, *B*) or ICAM-1 (Fig E12, *C*). **D** and **E**, Quantification of total intensity of perforin (Fig E12, *D*) and pVav-1 (Fig E12, *E*) at the IS. Error bars indicate ± s.d. Data represent 4 independent experiments.

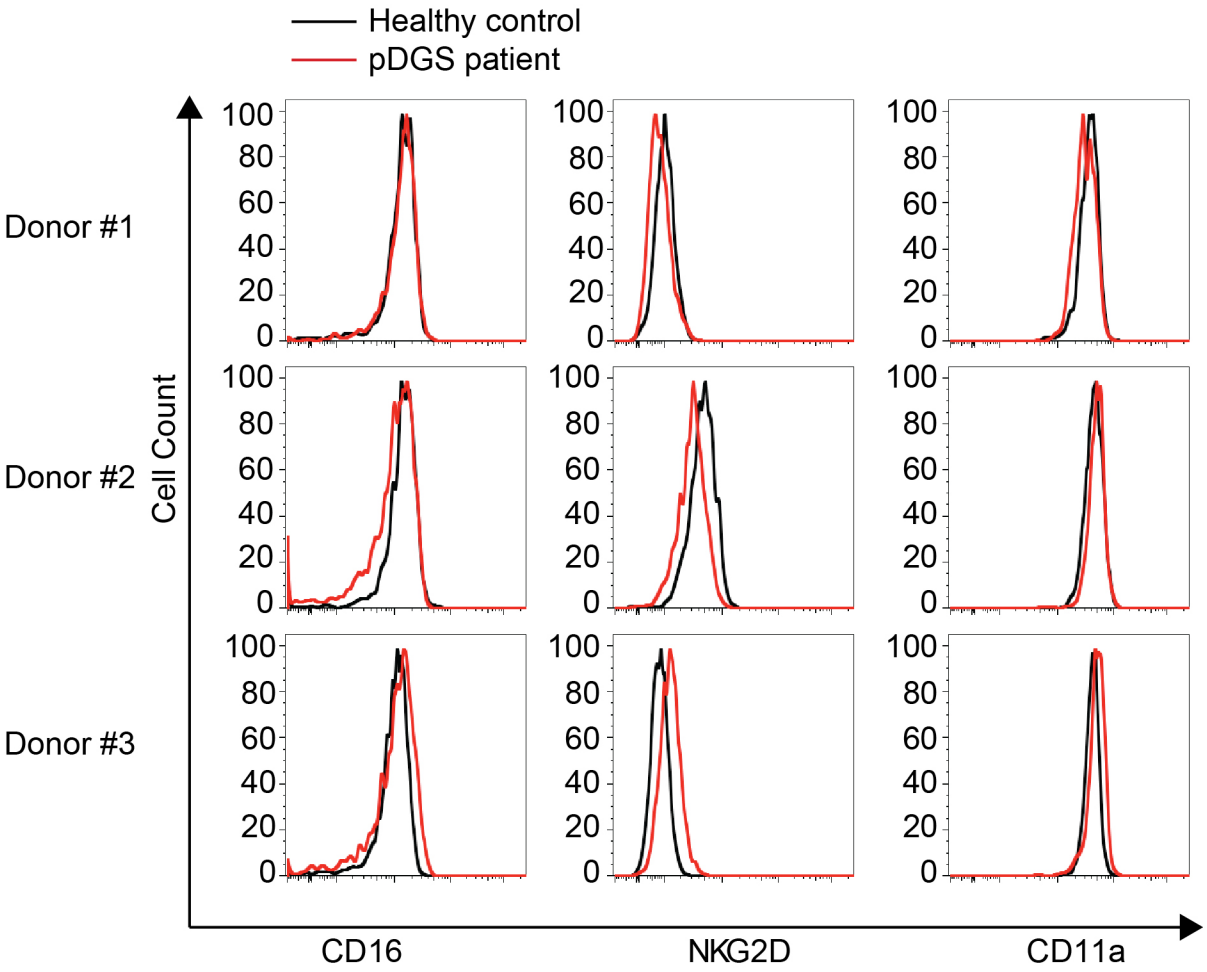

FIG E13. Comparable expression levels of activating receptors and integrin on NK cells from healthy controls and pDGS patients. FACS analysis of CD16, NKG2D and CD11a expression levels on NK cells from healthy control (black line) and pDGS patients (red). NK cells were gated on live $CD3^{-}CD56^{+}$ population. Data represents 3 independent experiments.

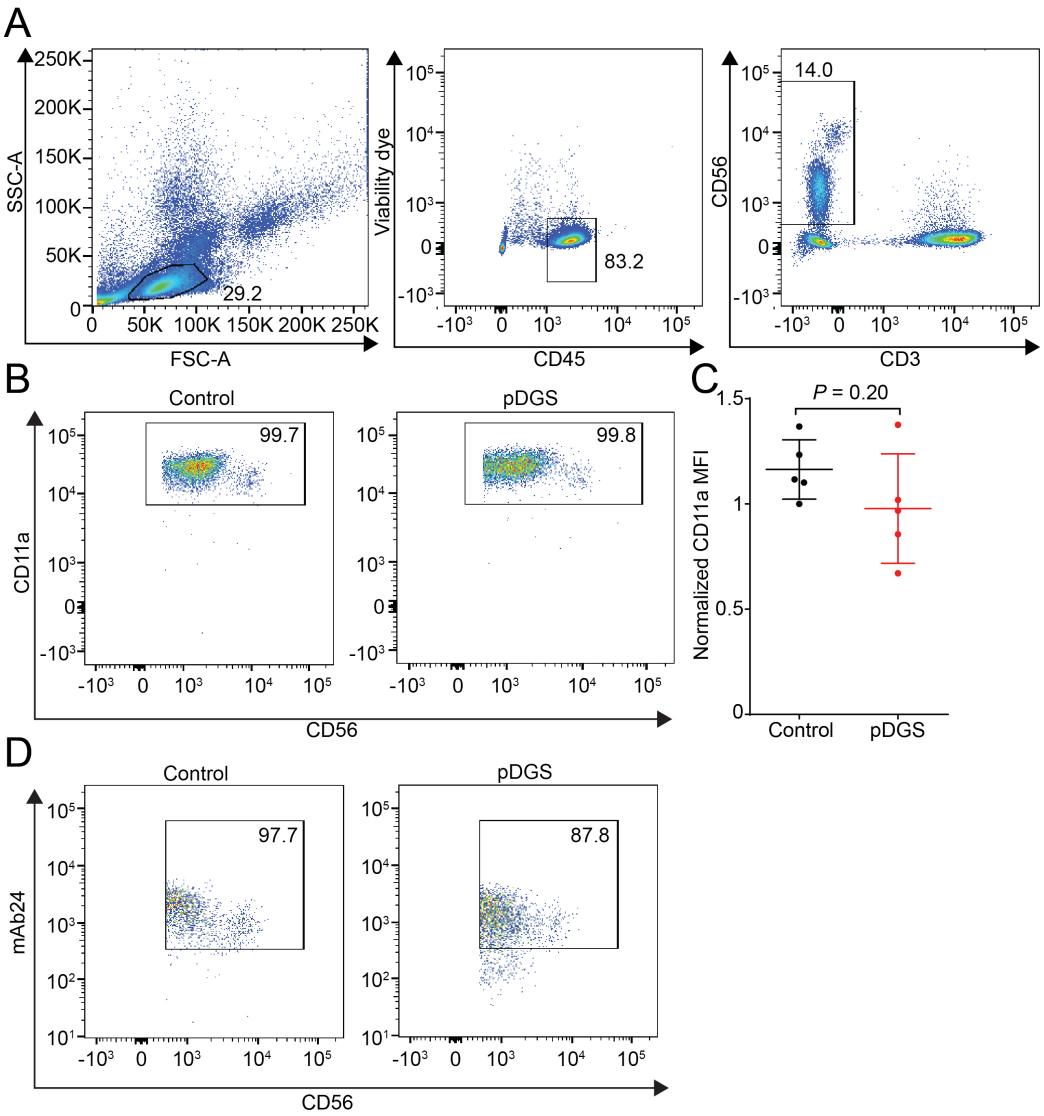

FIG E14. Comparable expression levels of total CD11a on NK cells from healthy controls and pDGS patients. A, Gating strategy of identifying NK cells in PBMCs. NK cells were gated on live $CD45^{+}CD3^{-}CD56^{+}$ cells from PBMCs. **B** and **C**, The

expression level of total CD11a on NK cells was defined by percentage (Fig E14, *B*) and MFI (Fig E14, *C*). **D**, The percentage of NK cells with activated LFA-1 ($mAb24^{+}$) in response to PMA and ionomycin. Data represent 4 independent experiments.

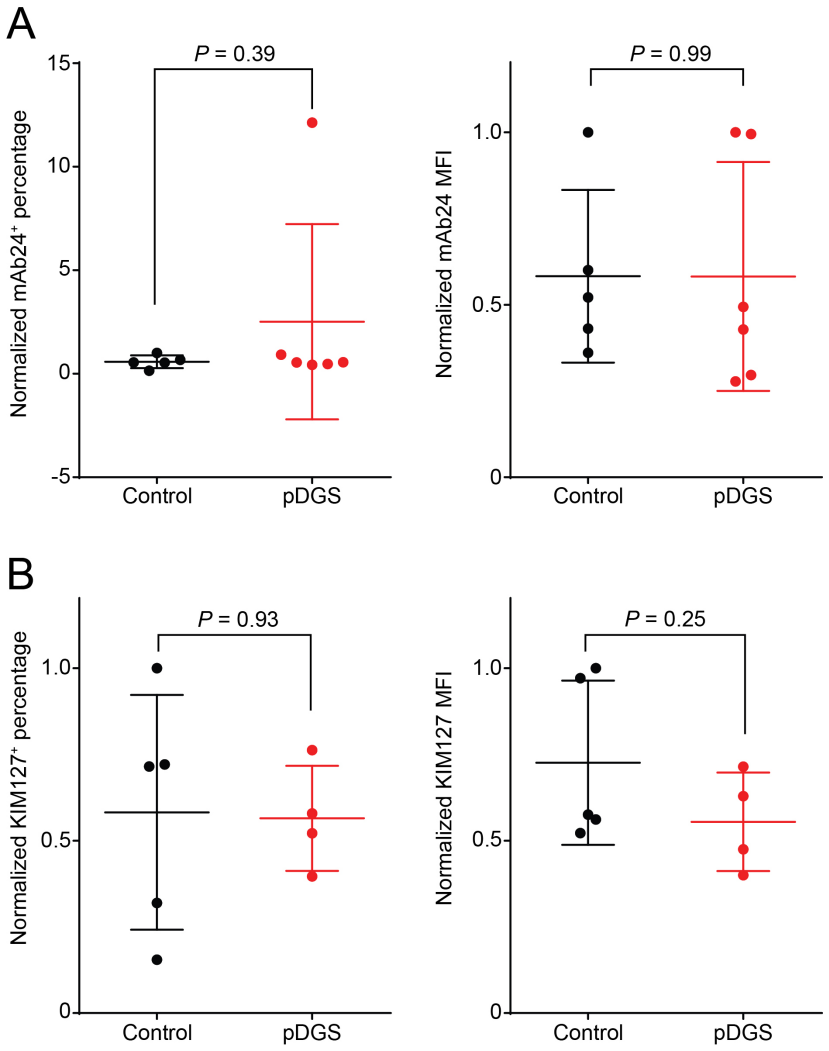

FIG E15. Comparable expression levels of activated LFA-1 in resting NK cells from healthy controls or pDGS patients.

A, The normalized percentage (left) and MFI (right) of activated (mAb24^{+}) LFA-1 in resting NK cells without stimulation *in*

vitro. Data are from 5 controls and 6 pDGS patients. **B**, The normalized percentage (left) and MFI (right) of intermediate ($KIM127^{+}$) LFA-1 in resting NK cells without stimulation *in vitro*. Data are pooled from 5 controls and 4 pDGS patients. Error bars indicate ± s.d.

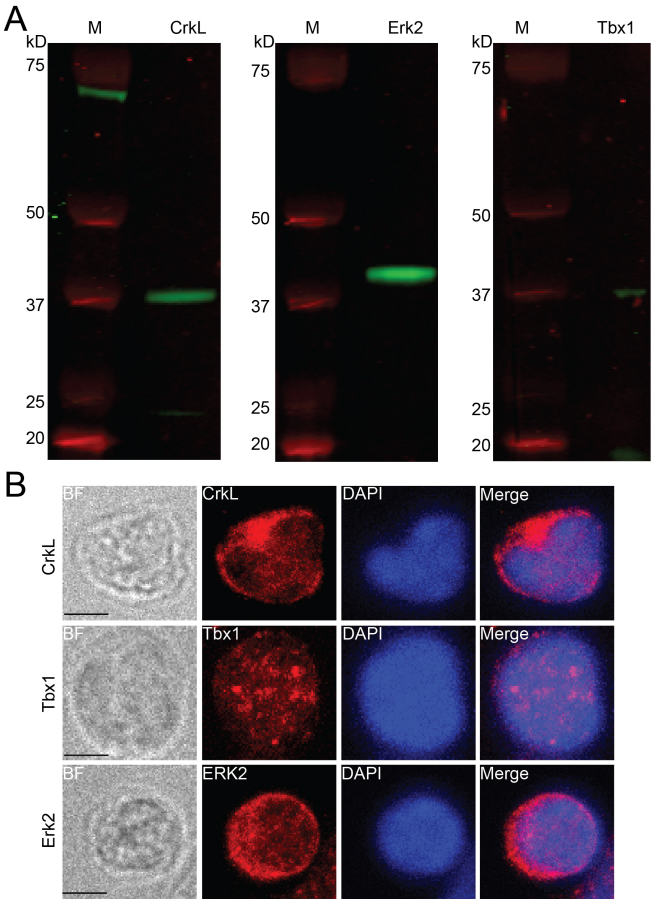

FIG E16. Validation of antibody specificity. A, Protein lysate from 4 x10^6 healthy PBMCs was probed with anti-CrkL or anti-Erk2 antibody. Lysate from 16 x10^6 healthy PBMCs were probed with anti-Tbx1 antibody. **B**, Confocal images showing CrkL, Tbx1 and Erk2 distribution in healthy PBMCs. Cells were fixed, permeabilized and stained with individual primary antibody followed by the corresponding fluorophore-conjugated secondary antibody. Scale bars represent 3.0 μm.

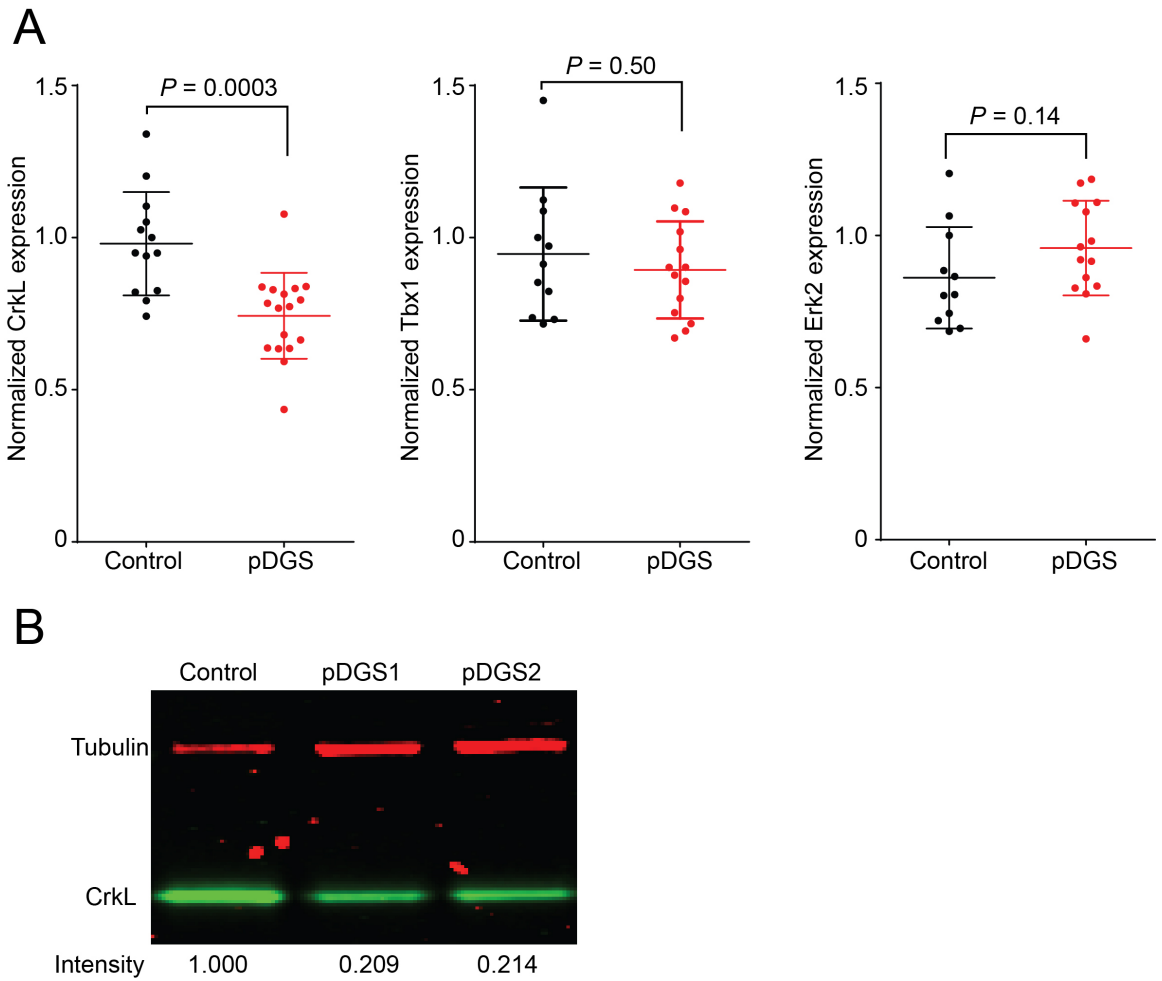

FIG E17. CrkL, Tbx1, and Erk2 expression in pDGS. **A**, FACS analysis of CrkL, Tbx1, and Erk2 expression in PBMCs from healthy control subjects (Control) and pDGS patients (pDGS). MFI were measured by flow cytometry. Error bars indicate ± s.d. Data are pooled from at least 11 controls and 14 pDGS patients. **B**, Western blotting of CrkL in healthy controls and pDGS patients (lysates from ~1x10^6 PBMCs). Note that Tbx1 is undetectable by Western blotting in both control and

pDGS patients (not shown). None pDGS patients carrying *Erk2* gene deletion in our cohort of 18 pDGS patients was noticed (not shown).

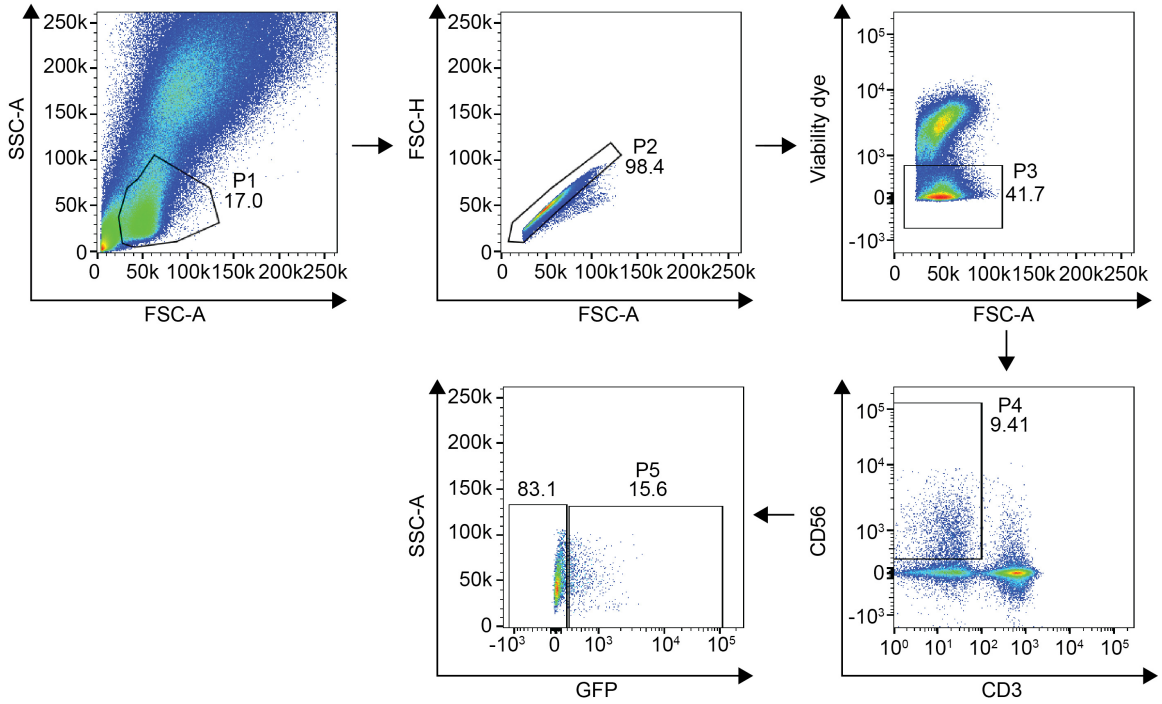

FIG E18. Gating strategy to identify primary NK cells transduced with CrkL-GFP lentivirus. Freshly isolated PBMCs were transduced with CrkL-GFP lentivirus. CrkL-GFP positive NK subsets in human PBMCs were sequentially gated on lymphocytes (P1), singlets (P2), live cells (P3), CD3-CD56+ (P4), and GFP+CD3-CD56+ cells (P5).

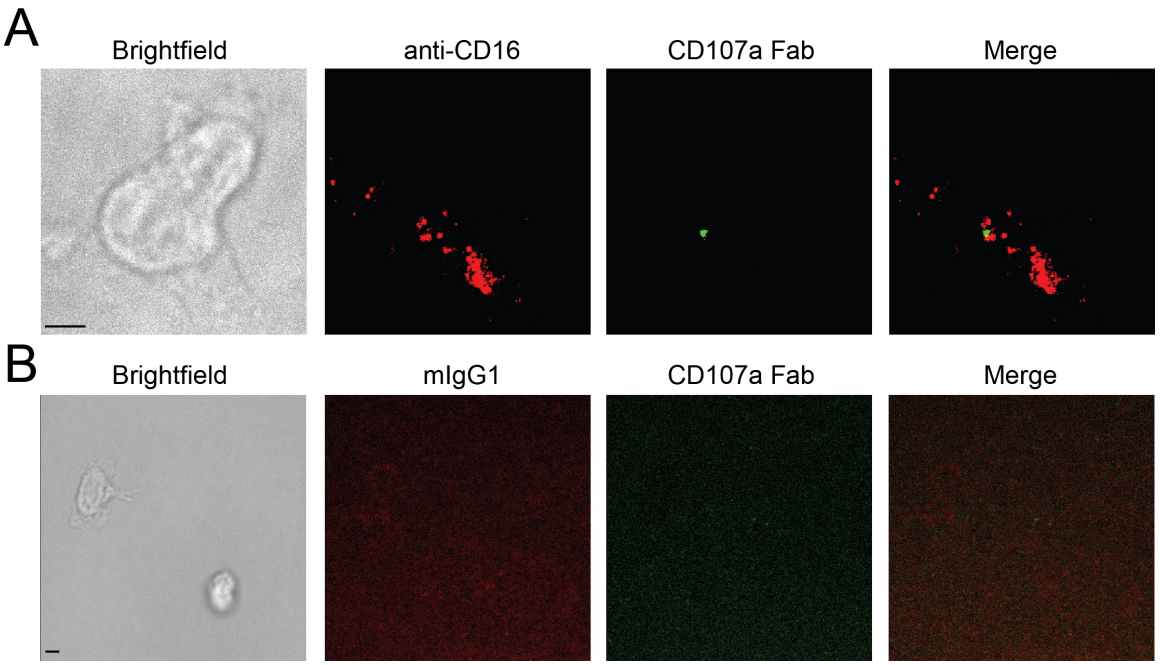

FIG E19. Degranulation elicited by lipid bilayer carrying anti-CD16, but not mouse IgG1 isotype control. A and **B**, Freshly isolated primary NK cells on bilayers carrying anti-CD16-Alexa Fluor 568 (Fig E19, A) or mouse IgG1-Alexa Fluor 568 isotype control (Fig E19, B). Cells were imaged by 3D confocal microscopy in the presence of anti-CD107a Fab-Alexa Fluor 647. Note that mouse IgG1 isotype control did not trigger NK cell degranulation and CD107a Fab-Alexa Fluor 647 did not label NK cells non-specifically. Scale bar represents 3 μm. Data from one experiment.

Table E1. Lymphocyte phenotyping of pDGS patients used in functional restoration assays

	Gender	Age (yr)	Genotype	ALC	$CD3^+$ (%)	$CD19^+$ (%)	$CD3^-CD56^+$ $CD16^+$ (%)	$CD3^+$ counts (cells/mm^3)	$CD19^+$ counts (cells/mm^3)	$CD3^-CD56^+$ $CD16^+$ counts (cells/mm^3)
P1	F	11	FISH	1194	57 (54-78)*	26 (11-25)	16 (7-28)	680 (1014-2557)	310 (204-703)	191 (152-595)
P2	M	8.5	CMA+ FISH	901	65 (54-78)	22 (11-25)	12 (7-28)	586 (1014-2557)	198 (204-703)	108 (152-595)
P3	F	0.6	FISH	3249	43 (48-76)	39 (12-39)	18 (3-14)	1397 (1919-5054)	1267 (566-2535)	585 (181-901)
P4	F	12.5	CMA	2381	53 (54-78)	37 (11-25)	8 (7-28)	1262 (1014-2557)	881 (204-703)	190 (152-595)
P5	F	11	FISH	2286	72 (54-78)	18 (11-25)	9 (7-28)	1646 (1014-2557)	411 (204-703)	206 (152-595)
P6	F	4	CMA	4522	51 (58-74)	26 (13-31)	17 (3-19)	2306 (1656-3841)	1176 (421-1397)	769 (123-785)
P7	F	6	CMA	3826	37 (56-76)	36 (11-28)	27 (5-21)	1416 (991-2997)	1377 (249-865)	1033 (128-474)
P8	F	5	CMA	1619	49 (56-76)	35 (11-28)	14 (5-21)	793 (991-2997)	567 (249-865)	227 (128-474)

* Normal age-matched ranges under each parameter. ALC: Absolute Lymphocyte Count, FISH: Fluorescence in situ hybridization, CMA: Chromosome microarray assay.

Figure E2: Clinical characteristic of pDGS patients used in NK cell functional assays

	Gender	ALC (normal range)	$CD3^+$ %, counts (normal range for age %, counts)	$CD3^-$ $CD56^+CD16^+$ (%, counts)	Autoimmunity	Infections	NC	ADCC	mAb 24^+ (%)	KIM 127^+ (%)	CD107 a^+ (%)
P1	F	1194 (1900-3700)	57%, 680 (54-78%; 1014-2557)	16%, 191 (7-28%; 152-595)	Thyroiditis, Chronic Urticaria*	Molluscum; Warts; recurrent URI			low	low	
P9	F	1299 (1400-3300)	57%, 740 (54-78%; 1014-2557)	17%, 221 (7-28%; 152-595)	None	Autism; recurrent URI			low	low	
P10	M	1836 (1900-3700)	54%, 991 (54-78%; 1014-2557)	17%, 312 (7-28%; 152-595)	None	Cellulitis; Dermatophytosis; Seborrheic Dermatitis; recurrent OM/URI			low		
P11	F	1830 (1900-3700)	54%, 988 (56-76%; 991-2997)	26%, 476 (5-21%; 128-474)	None	Asthma; URI	low	low	low		
P12	M	3037 (2300-5400)	59%, 1792 (56-76%; 991-2997)	11%, 334 (5-21%; 128-474)	None	Past EBV infection (not current), human Metapneumovirus (hospitalized 2013), OM	low	low	low	low	normal
P13	M	2389 (2300-5400)	42%, 1003 (56-76%; 991-2997)	19%, 454 (5-21%; 128-474)	None	Recurrent Pneumonia; recurrent OM/URI; Metapneumovirus virus (hospitalized 2014)	ND	ND			normal
P14	M	2665 (1900-3700)	45%, 1199 (56-76%; 991-2997)	36%, 959 (5-21%; 128-474)	None	Recurrent OM/URI, IgA deficiency**	ND	ND			normal
P15	M	6132 (3400-9000)	51%, 3128 (48-76%; 1919-5054)	15%, 920 (3-14%; 181-901)	None	Recurrent OM/URI; Aspiration Pneumonia	low	low			
P16	M	ND	ND	ND	None	Aspiration Pneumonia	normal	low			normal
P17	M	1268 (1900-3700)	65%, 824 (54-78%; 1014-2557)	10%, 127 (7-28%; 152-595)	Thyroiditis	OM/URI, recurrent; Metapneumovirus (hospitalized 2014)	low	low			normal
Pt 18	F	3377 (1000-2800)	70%, 2364 (58-88%; 798-2594)	13%, 439 (3-22%; 89-472)	None	Thoracic Herpes Zoster with dissemination outside dermatome, Contact Dermatitis with fungus infection	ND	ND	low	low	

	Thrombocytopenia, Chronic Sinusitis, ITP

Note: P1 cells were used in both NK cell restoration and functional assays. The 'low' and 'normal' in killing, mAb24/KIM127, and CD107a degranulation are defined by comparing individual patient values to the mean value of healthy controls. Normal age-matched ranges are presented under each parameter.
ALC: Absolute Lymphocyte Count; **NC**: Natural Cytotoxicity; **ADCC**: Antibody-dependent cell-mediated cytotoxicity; **OM**: Otitis media; **URI:** upper respiratory infection; **ND**: No Data; **EBV**: Epstein–Barr virus

* Cyclosporine therapy for severe chronic urticaria
** Co-existing IgA Deficiency (<10 mg/dL) diagnosed at 9 years of age

References

1. Driscoll DA, Budarf ML, Emanuel BS. A genetic etiology for DiGeorge syndrome: consistent deletions and microdeletions of 22q11. Am J Hum Genet 1992; 50:924-33.

2. Kobrynski LJ, Sullivan KE. Velocardiofacial syndrome, DiGeorge syndrome: the chromosome 22q11.2 deletion syndromes. Lancet 2007; 370:1443-52.

3. Gennery AR. Immunological aspects of 22q11.2 deletion syndrome. Cell Mol Life Sci 2012; 69:17-27.

4. Chinen J, Rosenblatt HM, Smith EO, Shearer WT, Noroski LM. Long-term assessment of T-cell populations in DiGeorge syndrome. J Allergy Clin Immunol 2003; 111:573-9.

5. Davis CM, Kancherla VS, Reddy A, Chan W, Yeh HW, Noroski LM, et al. Development of specific T-cell responses to Candida and tetanus antigens in partial DiGeorge syndrome. J Allergy Clin Immunol 2008; 122:1194-9.

6. Markert ML, Hummell DS, Rosenblatt HM, Schiff SE, Harville TO, Williams LW, et al. Complete DiGeorge syndrome: persistence of profound immunodeficiency. J Pediatr 1998; 132:15-21.

7. Markert ML, Boeck A, Hale LP, Kloster AL, McLaughlin TM, Batchvarova MN, et al. Transplantation of thymus tissue in complete DiGeorge syndrome. N Engl J Med 1999; 341:1180-9.

8. Tantibhaedhyangkul U, Davis CM, Noroski LM, Hanson IC, Shearer WT, Chinen J. Role of IL-7 in the regulation of T-cell homeostasis in partial DiGeorge syndrome. J Allergy Clin Immunol 2009; 123:960-2 e2.

9. Tison BE, Nicholas SK, Abramson SL, Hanson IC, Paul ME, Seeborg FO, et al. Autoimmunity in a cohort of 130 pediatric patients with partial DiGeorge syndrome. J Allergy Clin Immunol 2011; 128:1115-7 e1-3.

10. Jonas RK, Montojo CA, Bearden CE. The 22q11.2 deletion syndrome as a window into complex neuropsychiatric disorders over the lifespan. Biol Psychiatry 2014; 75:351-60.

11. Muldoon M, Ousley OY, Kobrynski LJ, Patel S, Oster ME, Fernandez-Carriba S, et al. The effect of hypocalcemia in early childhood on autism-related social and communication skills in patients with 22q11 deletion syndrome. Eur Arch Psychiatry Clin Neurosci 2014.

12. Alpert MD, Harvey JD, Lauer WA, Reeves RK, Piatak M, Jr., Carville A, et al. ADCC develops over time during persistent infection with live-attenuated SIV and is associated with complete protection against SIV(mac)251 challenge. PLoS Pathog 2012; 8:e1002890.

13. Paddison PJ, Cleary M, Silva JM, Chang K, Sheth N, Sachidanandam R, et al. Cloning of short hairpin RNAs for gene knockdown in mammalian cells. Nat Methods 2004; 1:163-7.

14. Zheng P, Kissler S. PTPN22 silencing in the NOD model indicates the type 1 diabetes-associated allele is not a loss-of-function variant. Diabetes 2013; 62:896-904.

15. Antoku S, Mayer BJ. Distinct roles for Crk adaptor isoforms in actin reorganization induced by extracellular signals. J Cell Sci 2009; 122:4228-38.

16. Herold MJ, van den Brandt J, Seibler J, Reichardt HM. Inducible and reversible gene silencing by stable integration of an shRNA-encoding lentivirus in transgenic rats. Proc Natl Acad Sci U S A 2008; 105:18507-12.

17. Barber DF, Faure M, Long EO. LFA-1 contributes an early signal for NK cell cytotoxicity. J Immunol 2004; 173:3653-9.

18. Bryceson YT, March ME, Barber DF, Ljunggren HG, Long EO. Cytolytic granule polarization and degranulation controlled by different receptors in resting NK cells. J Exp Med 2005; 202:1001-12.

19. Grier JT, Forbes LR, Monaco-Shawver L, Oshinsky J, Atkinson TP, Moody C, et al. Human immunodeficiency-causing mutation defines CD16 in spontaneous NK cell cytotoxicity. J Clin Invest 2012; 122:3769-80.

20. Theorell J, Schlums H, Chiang SC, Huang TY, Tattermusch A, Wood SM, et al. Sensitive and viable quantification of inside-out signals for LFA-1 activation in human cytotoxic lymphocytes by flow cytometry. J Immunol Methods 2011; 366:106-18.

21. Liu D, Peterson ME, Long EO. The adaptor protein Crk controls activation and inhibition of natural killer cells. Immunity 2012; 36:600-11.

22. Brian AA, McConnell HM. Allogeneic stimulation of cytotoxic T cells by supported planar membranes. Proc Natl Acad Sci U S A 1984; 81:6159-63.

23. Rak GD, Mace EM, Banerjee PP, Svitkina T, Orange JS. Natural killer cell lytic granule secretion occurs through a pervasive actin network at the immune synapse. PLoS Biol 2011; 9:e1001151.